Cladding Tube Testing in Creep Conditions under Multiaxial Loadings: A New Device and Some Experimental Results

Catherine Grosjean[1),2)], Dominique Poquillon[2)], Jean-Claude Salabura[2)], Jean-Marc Cloué[1)]

1) AREVA-NP Fuel – Design and Sales, Lyon, France
2) CIRIMAT, INP/ENSIACET, Toulouse, France

ABSTRACT

In order to carry out creep tests under multiaxial loadings and controlled environment, a new device has been designed and developed. It enables to test cladding tubes between 280 and 450°C with complex loadings paths obtained using controlled internal pressure and imposed tensile stress. Each parameter is independent. This paper first details the possibility of this device and its performances. Then, some experimental results of creep tests are presented. They were carried out on Zircaloy 4, which has already been largely studied previously [1, 2], allowing thus comparisons.

INTRODUCTION

Zirconium alloys are widely used for nuclear applications, especially for the production of cladding tubes. In order to improve design and lifetime of these structures, mechanical models have been developed. Therefore, to fit the model to reality, testing creep behavior of fuel claddings is essential. In service, these components are subjected to complex thermo mechanical loadings but also to other phenomena due to their environment: irradiation, oxidation...

Polycrystalline models dedicated to zirconium alloys have been developed [3, 4], taking into accounts the specific distribution of grain orientations which is optimized in cladding tubes because of its strong influence on the mechanical behavior [5]. But the development of these models has pointed out that the load path has a great influence on the strain rate and that further data were needed to achieve a good fit of the models. Indeed, because of the effect of fuel cycle, cladding tubes experience an increasing internal pressure. So, experiments have to be carried out under complex load paths in order to get relevant data. During these experiments, it is necessary to get strain evolution both in the axial direction and in the circumferential direction because of the texture of the tube and of the complexity of the loading. However studying load paths requires the control of loading conditions, and consequently the management of adapted experimental devices. Up to now, only “simple load” paths were characterized (tensile or biaxial tests). Thus, the first step was to design a new device to test cladding tube, without irradiation effects, but under various loading paths.

In the first part of this paper, we will introduce this new device, its components and its abilities before illustrating them with some creep tests results on a well studied zirconium alloy, Zircaloy 4.

THE NEW EXPERIMENTAL DEVICE

This new device have been developed and built in the CIRIMAT. It can be divided into five independent components: the tensile and compression test device, the sample, the laser extensometers, the lamps furnace and the pressure regulation system (Fig. 1).

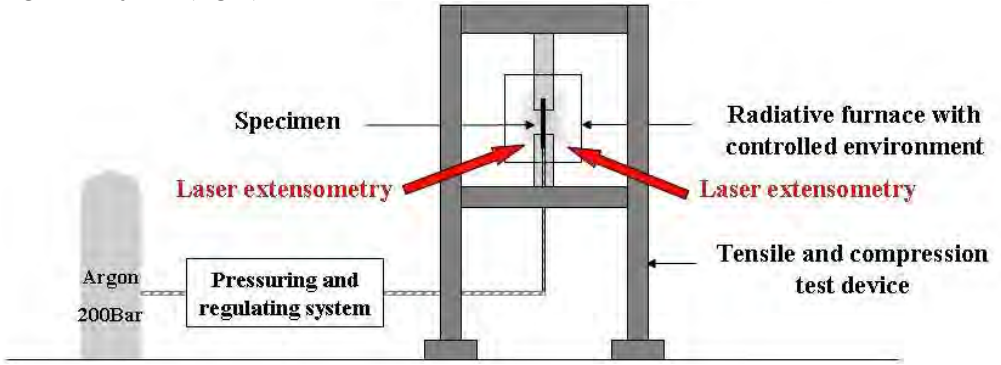

Fig. 1 : Scheme of the new device for multiaxial creep test.

First this system enables multiaxial loadings by pressuring the specimen (internal pressure up to 200 bars) and monitoring the axial force. The pressure subsystem is controlled independently from the tensile compression device allowing various loading paths. The axial loading on the specimen can reach 10kN. The regulation of the axial force is realized at ±2N through monitoring displacements of the crosshead of the tensile compression device. Furthermore, this load control is independent from the heating program. Thus, isothermal or an-isothermal mechanical solicitations can be achieved.

The samples tested on that device are 130 mm length zirconium alloy tubes. These tubes are gripped with a combination of inox plugs and Swagelock coupling device as detailed on Figure 2. This allows axial load up to 5000N and internal pressure up to 200 bars. Moreover a Zircaloy 4 core is introduced inside, both to reduce gas volume in the specimen to answer European legislation concerning devices under pressure [6].

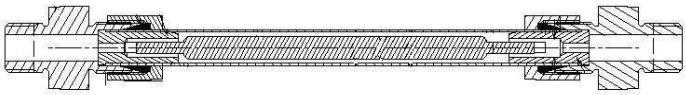

Fig. 2 : Sample and clamping set.

The study of the thermal creep behavior of these tubes used as cladding tube requires a furnace allowing high heating rate (5°C/s) but the main point is to limit the thermal gradient (±3°C) on the gauge length (30 mm in the center of the tube). A lamp furnace has been designed for these purposes. Tests have been realized under argon and the furnace achieves these goals. Between 260°C and 400°C the thermal gradients remain below 1°C during the whole creep test. That refinement comes from the use of several lamps located at different levels corresponding to distinct and independent zones, each of them being monitored by its own temperature regulator and thermocouple (Fig. 3). The thermocouples are spot-welded, the first one in the middle of the sample, and the two others on the limits of the gauge length. In that way, the power of each lamp can be continuously optimized in order to limit the thermal gradient.

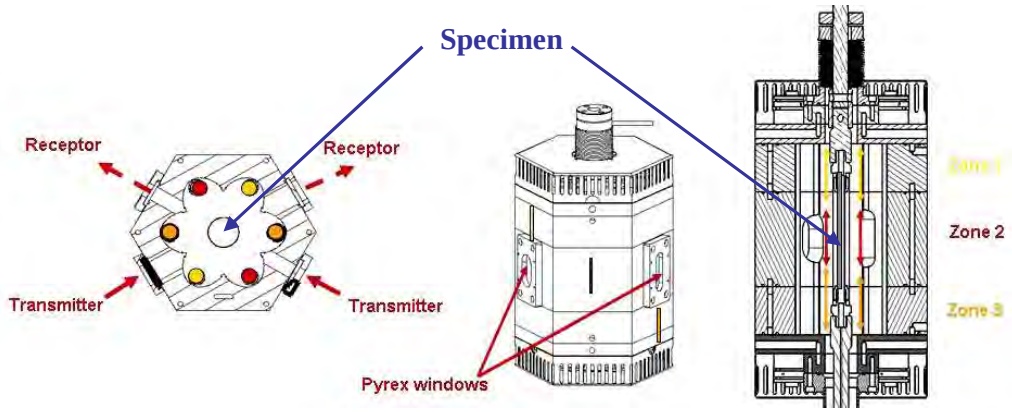

Fig. 3: Radiative lamps furnace.

The furnace was also designed to carry out creep test under control environment. Oxidation is prevented by using a controlled neutral gas flow inside the furnace chamber. Four Pyrex windows are located on the furnace in order to let the laser extensometers measure the stressed sample (Fig. 3).
Laser extensometers have been chosen for this device because they allow the measurement of the axial and diametric strain of the tube without contact. The system uses two couples of laser transmitter/receptor. The measure of the diameter variation is achieved directly by measuring the changes in the length of the intercepted part of the horizontal laser ply (Fig. 4). To measure axial deformations, the vertical laser transmitter sends a laser ply on two Alloy 718 flags spot-welded on the specimen delimiting the gauge length (Fig. 4).

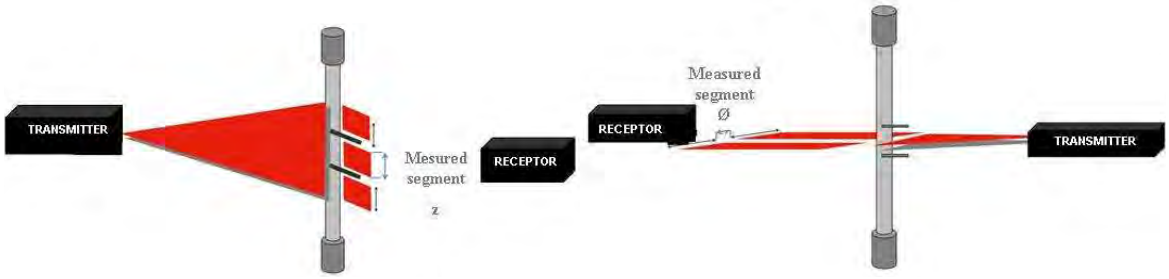

Fig. 4 : Laser extensometers used to measure axial and diametric dimensions variations.

The variation of this distance z (Fig. 4) is thus measured (with an accuracy of 1µm), and gives us the axial strain ε_{zz} as follows:

$$\varepsilon_{zz} = \ln(1+\frac{z-z_0}{z_0}) \quad (1)$$

The circumferential strain is deduced from the variation of the shadow of the tube (ϕ) on the horizontal laser receptor as follows:

$$\varepsilon_{\theta\theta} = \ln(1+\frac{\phi-\phi_0}{\phi_0}) \quad (2)$$

MATERIALS

The investigated zirconium alloy provided for creep test of cladding tube is Zircaloy 4. This material has been chosen for the qualification tests of the device because many tests are reported in the literature on its mechanical behavior. Consequently comparisons will be easy with our experimental data. The alloy chosen for the study is a stress-relieved Zircaloy 4. Its chemical composition is given Table 1.

Table 1 : Chemical composition of the investigated alloy (%wt)

Sn	O	Fe	Cr	S	Zr
1.20 - 1.50	0.1 - 0.15	0.18 - 0.24	0.07 - 0.31	0.001 - 0.0035	Bal.

The tubes present an outer diameter of 9.51 mm and an inner diameter of 8.35 mm. They have been formed by cold pilgering, which induces a strong crystallographic texture [7, 8]. Zirconium alloys are naturally anisotropic due to their hexagonal compact crystallographic structure. But the forming process enhances this strong anisotropy and modifes the mechanical behavior of the tubes [9]. As a consequence, loading paths strongly influence the mechanical response of the material. The device presented in the first part of this paper was built to get a better understanding of this point.

EXPERIMENTAL PROCEDURE

This procedure has been established and improved during various tests and depends on the biaxiality of the test. The results detailed here are only isothermal creep tests. All the tests have been performed under argon (internal pressure and furnace chamber) in order to avoid oxidation phenomena. First the sample is warmed until 400°C with a heating rate of 50°C/min. To avoid buckling during this step, a small axial load is imposed corresponding to a 3MPa axial stress. Then, when the temperature is stable (few minutes of soak time) with a thermal gradient below 3°C, the sample is submitted to the chosen mechanical loading (Fig. 5). For uniaxial creep test, an increasing load is applied at a given strain rate up to the chosen axial creep stress. For multiaxial creep tests requiring pressurization, there is one more step before heating. First the sample is submitted to a low pressure of 20 bars to check the pressure stability of the system (air tightness of the grips on the tube). Then, the furnace is settled to allow the heating up to 400°C. During heating, to avoid buckling, a small axial load is also imposed corresponding to a 3 MPa axial stress. As soon as the temperature is stabilized, the creep loading is imposed by monitoring both internal pressure and axial load up to the chosen values (Fig. 5).

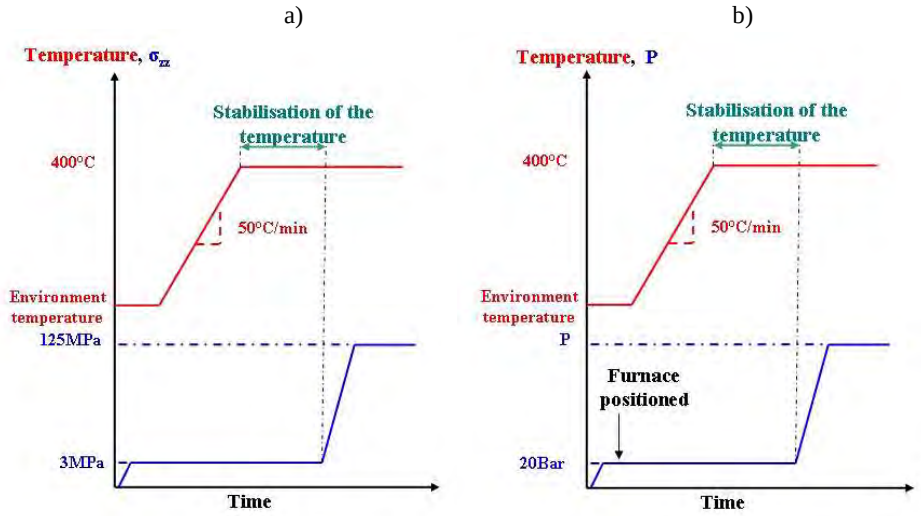

Fig. 5: Examples of mechanical and thermal loadings procedures. a) uniaxial creep test b) creep test under pressure

During the heating, the laser extensometers give indication of the axial and diametric coefficient of thermal expansion. During the isothermal mechanical loadings, data are collected to understand the elasto-viscoplasic behavior of the tubes.

RESULTS

Thermal results

The furnace tests were successful as from 280 to 400°C the thermal gradients in the gauge length remained below 1°C. Moreover the chosen temperature was obtained without notable delay or overshoot due to the use of lamps (Fig. 6). Indeed the temperature of the furnace only presented a delay of few degrees compared to the target temperature under 50°C. This point can be explained by the heating mode (radiation). But the delay decreases as soon as temperature increases. Then, concerning the "overshoot" at the end of the heating, this represents 2 or 3°C more than the target temperature. This overshoot disappears in less than 3 minutes.

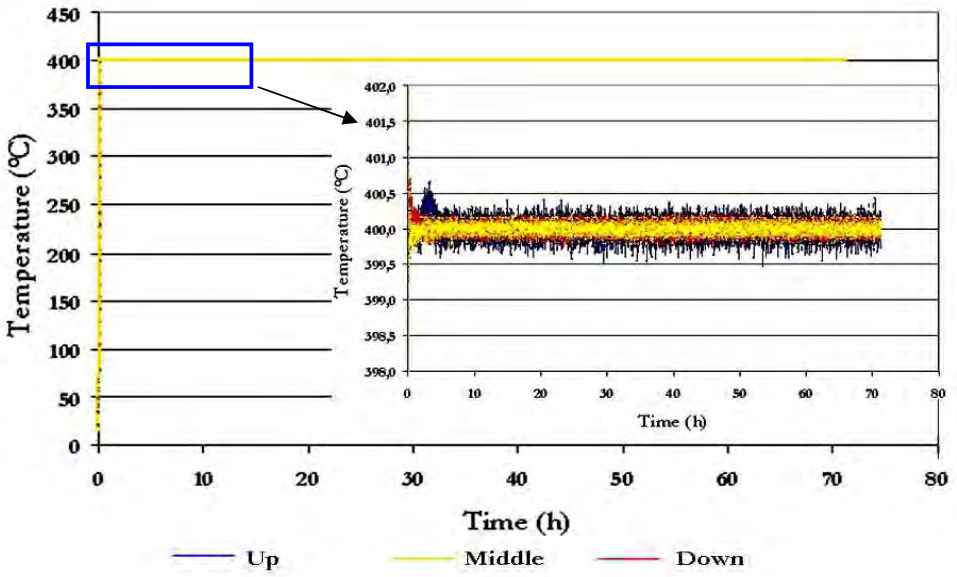

Fig. 6: Evolution of the temperature during a test (example of the test 2).

Then the study of the behavior of the tube during the heating enhances the anisotropy of dilatation. Indeed the circumferential thermal expansion is higher than the axial one for all the tests carried out in this study (Table 2). The ratio between these thermal expansion coefficients is close to 0.6. The average value of the coefficient of thermal expansion is 5.1 $10^{-6}K^{-1}$ in the axial direction, and 8.3 $10^{-6}K^{-1}$ in the circumferential direction. These values will be discussed later.

Table 2 : Results of the different tests carried out on Zy-4 tubes (NC: data non collected)

Test label	$\sigma_{\theta\theta}$ (MPa)	σ_{zz} (MPa)	$\dot{\varepsilon}$ (s^{-1})	20-400°C		Secondary creep		
				$\alpha_{\theta\theta}$ (K^{-1})	α_{zz} (K^{-1})	$\dot{\varepsilon}_{\theta\theta}$ (s^{-1})	$\dot{\varepsilon}_{zz}$ (s^{-1})	r
1	0	125	10^{-3}	8.97 10^{-6}	5.13 10^{-6}	-1.53 10^{-9}	3.55 10^{-9}	-2.32
2	0	125	10^{-3}	8.06 10^{-6}	4.79 10^{-6}	-1 16 10^{-9}	3.99 10^{-9}	-3.44
3	0	125	10^{-4}	7.58 10^{-6}	5.53 10^{-6}	-2.37 10^{-9}	4.51 10^{-9}	-1.90
4	0	125	10^{-4}	9.14 10^{-6}	5.67 10^{-6}	-3.86 10^{-9}	4.06 10^{-9}	-1.06
5	0	125	10^{-6}	8.73 10^{-6}	5.62 10^{-6}	-2.99 10^{-9}	4.73 10^{-9}	-1.58
6	0	125	10^{-6}	6.77 10^{-6}	5.13 10^{-6}	-1.92 10^{-9}	3.90 10^{-9}	-2.03
7	80	160	10^{-6}	NC	NC	1.28 10^{-8}	1.27 10^{-8}	0.99
8	80	160	10^{-6}	7.67 10^{-6}	5.58 10^{-6}	1.80 10^{-8}	1.94 10^{-8}	1.08
9	120	120	10^{-6}	8.17 10^{-6}	3.94 10^{-6}	3.52 10^{-8}	1.57 10^{-8}	0.45
10	120	120	10^{-6}	NC	NC	2.94 10^{-8}	1.23 10^{-8}	0.42
11	140	70	10^{-6}	8.55 10^{-6}	5.43 10^{-6}	5.47 10^{-8}	9.81 10^{-9}	0.18
12	140	70	10^{-6}	7.50 10^{-6}	4.19. 10^{-6}	7.89 10^{-8}	7.89 10^{-9}	0.25
13	138	38	10^{-6}	6.87 10^{-6}	5.03 10^{-6}	6.46 10^{-8}	6.03 10^{-9}	0.09
14	138	35	10^{-6}	NC	NC	6.57 10^{-8}	8.11 10^{-9}	0.12

Mechanical behavior

The main point to note is the possibility to monitor independently pressure, axial load and temperature. Fourteen creep tests have been carried out under argon at 400°C with different biaxiality ratios (Fig. 7). Most of then were duplicated.

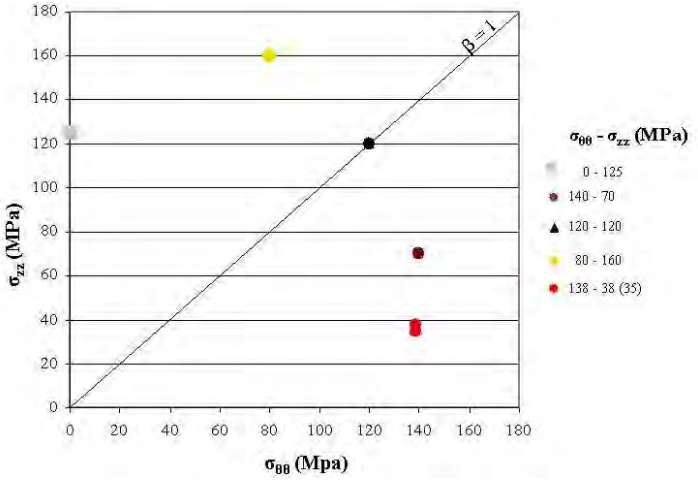

Fig. 7 : Map (axial stress versus hoop stress) of the stress states tested at 400°C under argon.

For uniaxial tests performed at 125 MPa (tests 1 to 6), different strain rates have been tested ($10^{-3}s^{-1}$, $10^{-4}s^{-1}$ and $10^{-6}s^{-1}$). As shown in Table 2, the loading rate has a small influence on the creep behavior (see also Fig. 8). For tests carried out with internal pressure (with or without additional axial loading), hoop strain and axial stress are controlled during the loading path. First, during the heating, they remain small (20 bars and 3 MPa) then proportional loading is imposed. For the stress levels of this study, the strains collected during mechanical loading remained elastic. Viscoplastic behavior was evidenced during the dwell time. Figure 8 is an example of biaxial creep strain measurement for tests 4 and 12. Tests were performed until stabilization of creep rate in order to determine axial and hoop strain rates in these conditions. These values are given in table 2 and plotted (absolute value) on Figure 9.

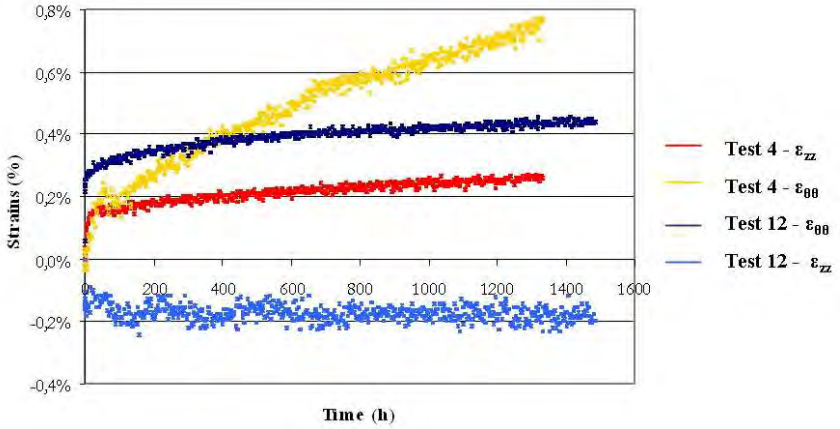

Fig. 8 : Strains versus time for a uniaxial and a biaxial creep test.

The strain anisotropy during secondary creep is measured with r ratio equals to $\frac{\dot{\varepsilon}_{zz}}{\dot{\varepsilon}_{\theta\theta}}$. It remains quite constant for a stress state. However, it is also interesting to use another type of plot to analyze theses creep results. Figure 10 shows a graph with a representation of the vectors of the creep strain rate (secondary creep) plotted for the different stress states tested.

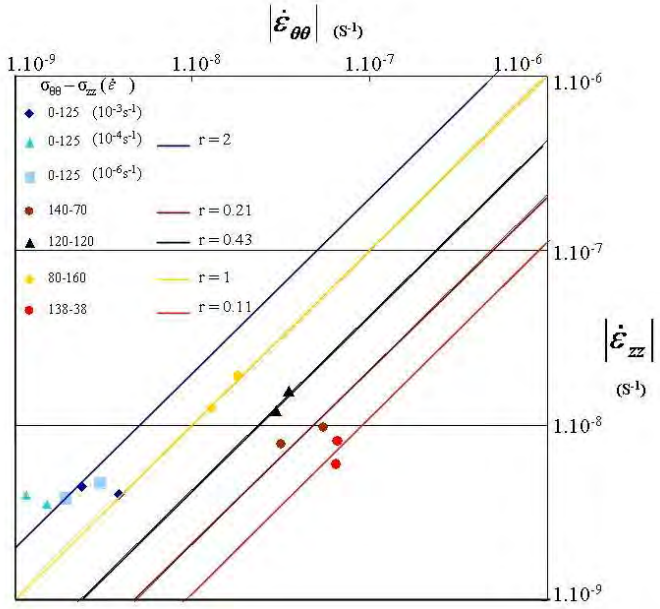

Fig. 9 : Map of the axial strain rate versus hoop strain rate (absolute value) during stationary creep for different stress states (see Fig. 7).

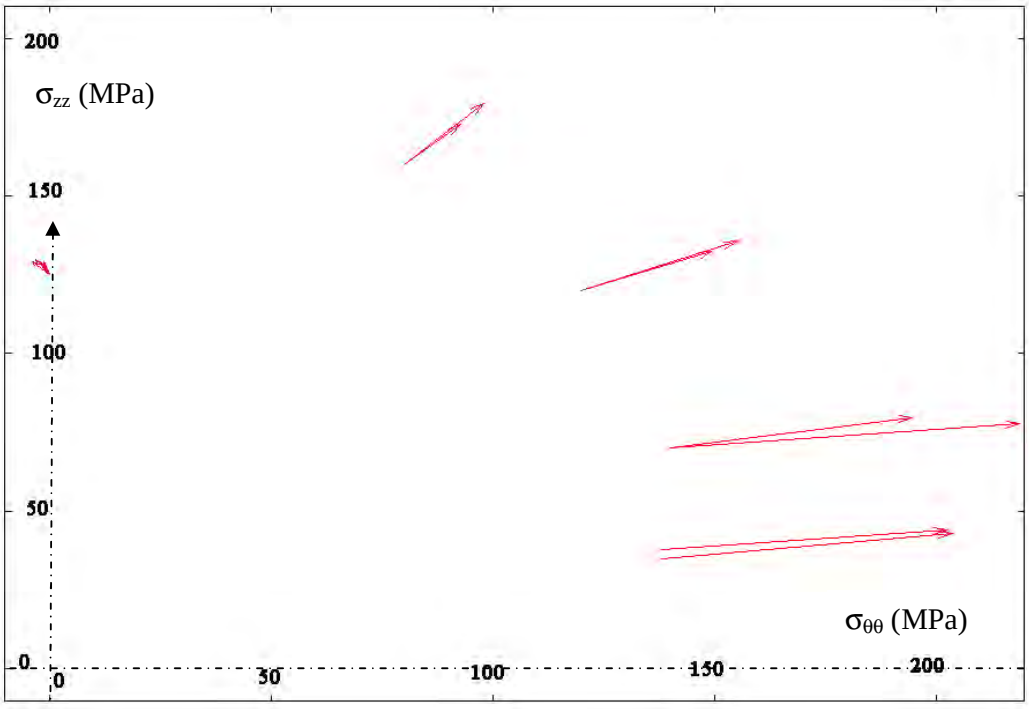

Fig. 10 : Representation of the vectors of the creep strain rate (secondary creep) plotted for the different stress states tested (see Fig. 7). The arrows size is proportional to the creep strain rate.

This graph shows that the cladding tube tested presents a very anisotropic behavior which depends highly of the biaxiality ratio ($\frac{\sigma_{zz}}{\sigma_{\theta\theta}}$ = ∞, 2, 1, 0.5, 0.27 or 0.25). For uniaxial test ($\frac{\sigma_{zz}}{\sigma_{\theta\theta}}$ => ∞), ratios between axial and hoop strain rates are always close to r=-2. The small value of the hoop strain rate can lead to uncertainty and it strongly affects the calculation of r. However the reproducibility of the tests is quite good. The other loading conditions induce higher rates and a better reproducibility. The arrows on Figure 10 evidence the yield surface shape and highlight the anisotropy of the Zircaloy 4 in creep conditions. Indeed for isotropic materials, the ratio r is well determined [10]. In the creep tests of this study, these ratios r are close but not equal to these specific values. More tests are needed to plot iso-creep-strain rate surface and to model anisotropy effect during stationary creep. Other tests are still in progress.

DISCUSSION

The furnace allows us to achieve creep tests in very good conditions: high heating rate and small thermal gradients are obtained on the gauge length. Furthermore, conditions remain stable during hours up to days. The new device is now tested, allowing us to realize various thermo-mechanical loadings on cladding tubes, under controlled atmosphere. As the pressure, the axial force and temperature are monitored in independent ways, the influence of each parameter can be explored. Up to now, tests were realized with a constant quantity of argon in the closed tube, without any possibility to control the hoop stress during the test (and during the heating). The qualification of the device presented in this article shows that complex loading paths are now possible in a large range of temperature. Laser extensometers offer a good accuracy in the measurement and the reproducibility of the creep tests is very good even for small creep rate. The strong anisotropy of the creep behavior of the tested materials is well established and more tests are required before modeling it. Creep tests under internal pressure can be compared to Brenner's results [12]. Indeed, he observed r ratios of 0.20 and 0.22 for respectively hoop stress of 113 MPa and 130 MPa. In the present study we found 0.18 and 0.25 (for hoop stress of 140 MPa). However these first results need to be confirmed.

Concerning the coefficients of thermal expansion, the values obtained on this new device can be compared with those observed by Brachet [11]. Indeed, for a zirconium-based alloy tube (Zr > 98%), the dilatometric measurements ranged from $5.58.10^{-6}K^{-1}$ up to $8.31.10^{-6}K^{-1}$ depending upon the cutting direction of the sample, for temperature between 200°C and 500°C. Our results are in good agreement with these values.

CONCLUSION

The new device developed for cladding tube testing offers large possibilities of loadings. The first results presented in this paper prove the variety of the tests that could be achieved in the future. New tests are in progress to get data at different stress levels and for different stress biaxilities. The effects on the creep behavior not only of the loading strain rate, but also of the loading path are going to be investigated. These new data are necessary to improve polycrystalline models used to predict the mechanical behavior of zirconium alloys under thermal creep conditions.

NOMENCLATURE

$\sigma_{\theta\theta}$ = circumferential stress, $\varepsilon_{\theta\theta}$ = circumferential strain; $\dot{\varepsilon}_{\theta\theta}$ = axial strain rate

σ_{zz} = axial stress, ε_{zz} = axial strain, $\dot{\varepsilon}_{zz}$ = circumferential strain rate

z = distance between the Alloy 718 flags and z_o = distance before heating and loading

ϕ = diameter of the tube with ϕ_0 = diameter of the tube before heating and loadings

REFERENCES

1. Signorelli, J. W., Loge, R. E., Chastel, Y B and Lebensohn, R. A., "Parameter identification method for a polycrystalline viscoplastic selfconsistent model based on analytical derivatives of the direct model equations," Modelling and Simulation in Materials Science and Engineering, 2000, Vol. 8, pp.193-209.
2. Gilormini, P. and, Ponte Castaneda P., "Accurate estimates for the creep behaviour of hexagonal polycristals," Acta Materialia, 2001, Vol. 49, pp. 329-337.
3. Miller, A K. "Unified constitutive equations for creep and plasticity", 1987.
4. Brenner, R., Béchade, J.L., Castelnau, O. and Bacroix, B. "Thermal creep of Zr–Nb1%–O alloys: experimental analysis and micromechanical modeling," Journal of Nuclear Materials, 2002, Vol. 305, pp. 175-186.
5. Delobelle, P.,Robinet, P., Geyer, P. and Bouffioux, P. '"A model to describe the anisotropic viscoplastic behaviour of Zircaloy-4 tubes," Journal of Nuclear Materials, 1996, Vol. 238, pp.135-162.
6. Equipements sous pression, Vol. DE 97.23.CE, 1997, p.21.
7. Kaddour, D. "Fluage isotherme et anisotherme dans les domaines monophasés (alpha et béta) et biphasés (alpha + béta) d'un alliage Zr-1%NbO," Ecole Nationale des Mînes de Paris, 2004.
8. Charquet, D. "Propriétés du zirconium et du hafnium,". Techniques de l'ingénieur, 1985.
9. Fundenberger, J. J., Wagner F., and Esling C., "Modelling and prediction of mechanical properties for materials with hexagonal symmetry (Zinc, Titanium and Zirconium alloys)," Acta Materialia, 1997, Vol. 45, pp. 4041-4055.
10. Pineau, A., Zaoui, A. and François, D. "Comportement mécanique des matériaux," Hermes, Paris, 1995.
11. Brachet, J.C., Castaing, A., Le Blanc, L., and Jouen, T., "Relationship between crystallographic texture and dilatometric behaviour of a hexagonal polycrystalline material," Materials Science Forum, 1998, Vol 273, p. 275-529.
12. Brenner R. "Influence de la microstructure sur le comportement en fluage thermique d'alliages de zirconium: analyse expérimentale et mise en œuvre de méthodes d'homogénéisation," Université Paris XIII, 2001.